Dyes and Pigments 239 (2025) 112733

Contents lists available at ScienceDirect

Dyes and Pigments

journal homepage: www.elsevier.com/locate/dyepig

Rapid chromatic alteration of Street Art: Mechanisms of deterioration of the painting materials of the *20 years of Freedom and Democracy* mural

Nicolò Guarnieri [a], Alessia Di Benedetto [b], Daniela Comelli [b], Francesco Mirani [c], David Dellasega [c], Laura Pagnin [a], Sara Goidanich [a,*], Lucia Toniolo [a]

[a] Department of Chemistry, Materials and Chemical Engineering, Politecnico di Milano, Piazza Leonardo da Vinci 32, 20133, Milan, Italy
[b] Department of Physics, Politecnico di Milano, Piazza Leonardo da Vinci 32, 20133, Milan, Italy
[c] Department of Energy, Politecnico di Milano, Piazza Leonardo da Vinci 32, 20133, Milan, Italy

ARTICLE INFO

Keywords:
Street art
Colour fading
Paints
Organic pigments
Hyperspectral imaging
FE-SEM
μ-ATR FTIR and μ-Raman

ABSTRACT

Over the last few years, contemporary mural paintings have gained significant importance as both artistic and social expressions within urban environments. The study focuses on the characterization of the faded painting materials from a case study in Milan, *20 years of Freedom and Democracy,* and its aesthetic, morphological and chemical alterations. The goal is to study the phenomenon of chromatic alteration and understanding causes and mechanisms. In this work, a diagnostic study based on non-destructive and micro-destructive investigation methods is presented, improving and integrating the knowledge about Street Art deterioration. The colour fading of this mural was clearly evident from the available online photographic documentation, which allowed the reconstruction of the evolution of its appearance over time since its realization. The analysis revealed that colour fading occurred within the first two years. A wide range of analytical techniques were employed to gain deeper insights into the qualitative and semi-quantitative composition of the materials. These included hyperspectral imaging, microscopy observations and molecular and elemental spectroscopies of collected paint samples (μ-FTIR ATR and reflectance mapping, μ-Raman spectroscopy, FE-SEM observation and EDXS mapping). Colour fading was found to affect less than 10 μm of the surface. The deterioration of the polymeric binder promotes the loss of pigments and therefore the enrichment of white fillers on the surface, the so-called chalking effect, in agreement with other studies on Street Art murals. Furthermore, the photochemical instability of specific pigments (PR112, C.I.:12370 and PY83, C.I.:21108) was demonstrated, leading to the dramatic colour changes observed on the real surface.

1. Introduction

Nowadays Street Art, like traditional mural paintings in the past, is gaining increasing cultural and social importance, in different urban contexts around the world. Emerged as rebellion and protest-driven movement in '60s, Street Art evolved into Urban Art in the '80s, shifting its focus towards social issues, ethical values and urban lifestyles [1,2]. Now recognized as a legitimate form of artistic expression, contemporary muralism creates large-scale artworks that enhance and revitalise urban spaces, particularly in socially challenged or economically depressed areas [3]. These murals are appreciated not only for their aesthetic appeal, but also for their ability to foster community identity and pride [4]. Today, artworks by renowned artists (e.g. Keith Haring, Blu, Banksy, Millo) are recognized as part of the contemporary artistic heritage and pose challenges in terms of protection and conservation, even though they are sometimes created without authorization [5–9]. Despite their increasing presence and importance, the conservation of these murals is not yet a common or shared practice, but remains a challenge [1,3]. The characterization of Street Art paintings and the assessments of their conservation state have been investigated in previous studies, both in real case studies [10–18] and through simulated mock-up experiments [5,19–23]. Contemporary murals are mainly created using synthetic paints based on acrylic and styrene-acrylic, alkyd or vinyl resins, chosen by artists for their vibrant colours and

* Corresponding author.
E-mail addresses: nicolo.guarnieri@polimi.it (N. Guarnieri), alessia.dibenedetto@polimi.it (A. Di Benedetto), daniela.comelli@polimi.it (D. Comelli), francesco.mirani@polimi.it (F. Mirani), david.dellasega@polimi.it (D. Dellasega), laura.pagnin@polimi.it (L. Pagnin), sara.goidanich@polimi.it (S. Goidanich), lucia.toniolo@polimi.it (L. Toniolo).

https://doi.org/10.1016/j.dyepig.2025.112733
Received 20 November 2024; Received in revised form 20 February 2025; Accepted 26 February 2025
Available online 27 February 2025

ease of application via spray, brush, or roller techniques [1,24–26]. The typical pigments employed in this kind of paint include both organic (e.g. phthalocyanine, azo, dioxazine) and inorganic compounds (e.g. calcite, titanium white in rutile and anatase phase, barium sulfate, gypsum). While organic pigments provide vivid colours, many of them exhibit very low durability in outdoor conditions. Several studies [11–16,19,23] highlight the significantly limited stability of these paintings in outdoor environments. In fact, the aesthetic, chemical-physical and mechanical properties of contemporary murals tend to deteriorate rapidly when exposed to environmental factors such as sun light, temperature fluctuation, humidity, rain water, pollutants, fine particulate matter, and micro-biological agents [1,2,8,27]. Additionally, other key factors contributing to their poor durability include: case-specific solar exposure, micro-climatic and pollution conditions, and the artist's modification of materials and application methods, which often do not follow manufacturer recommendation or proper substrate preparation procedures [1,10,14,16,17,23,26–31].

Among the various degradation patterns affecting these artworks [1,5,20,24,27,32,33], colour instability is particularly critical and appears to be a characteristic decay phenomenon. Chromatic alterations, indeed, have a high impact on the aesthetic appearance of murals, sometimes completely compromising their readability due to severe colour fading occurs [5,10,15,23,29,30]. Many authors have investigated colour fading and whitening (or chalking effect) in important case studies [10,15,16], formulating hypotheses about material degradation processes, which are primarily associated with photooxidative reactions occurring in the presence of UV solar radiation and atmospheric O_2. Some studies indicate that these are surface phenomena affecting only the outermost part of the painting layers (approximately 10 μm) [16,32,33]. The chalking effect is linked in the literature to the photolysis of the binder and the presence of inorganic fillers and white pigments [5,16,19,29,32,34]. Inorganic pigments, generally more stable than the organic ones, are often added to serve as fillers and extenders in paints. However, it has been observed that these compounds can cause problematic effects due to migration and/or local enrichment phenomena [1,17,20,23,33,35].

This paper investigates the contemporary mural "*20 Years of Freedom and Democracy*" located in Milan downtown, as a very interesting case to explore the colour fading. Situated in a highly polluted urban environment, the artwork has suffered drastic colour changes and severe deterioration. The selection of this mural was also driven by the of Milan municipality's intention to conserve and restore the painting, as well as by the careful attention of an expert conservator.[1]

A wide range of analytical techniques was employed to determine the qualitative and semi-quantitative changes in the painting materials, aiming to achieve a deeper understanding of the degradation phenomena. The painting was investigated through an integrated not- and micro-invasive approach, set-up in accordance with current literature [16,26,36], to identify the type of deterioration phenomena and their chemical –physical mechanisms. The ability to analyse complex mixture of inorganic and organic compounds, chieve high detection limits, and provide spatial resolution was crucial in addressing such complex challenges.

The combined use of microscopy and vibrational spectroscopy on micro-samples, along with the elaboration of VIS-reflectance imaging, proved to be the most effective strategy. The analytical techniques included hyperspectral imaging, optical microscopy, FE-SEM observation, and EDXS mapping and μ-FTIR (μATR and reflectance mapping), μ-Raman spectroscopy.

1.1. Case study - "20 Years of freedom and democracy"

The contemporary mural named "*20 Years of Freedom and Democracy*", also known as "*UBUNTU*", was created in Milan in July 2014 (Fig. 1). This artwork was painted by four artists: Nais (who depicted the woman on the left), Pao (artist of the figures at the centre-left), Ivan Tresoldi (creator of the writings at the centre) and Orticanoodles (who portrayed Mandela's face on the right). Commissioned by the municipality of Milan with support from the South African government and private companies, the mural celebrates South Africa's democracy and the coexistence of different people and cultures [37–39]. The section of the mural featuring Mandela's face has suffered the most important colour fading. This is mainly due to its stronger exposure to solar radiation compared to the rest of the mural, as a nearby building partially shades other sections during the day. The mural is located on a south perimetral wall (45°29′02.5"N and 9°10′34.6"E), facing on a street with an intense level of traffic. Fig. 1 compares of the aesthetic appearance of the mural immediately after the realization in 2014 (Fig. 1a) and in 2022 (Fig. 1b), highlighting how the chromatic appearance of the paints has changed, particularly in the areas depicting Mandela's face. Despite some localized small lacunae, cracks, and scratches in the paint layers - likely due to high human interaction and accessibility - the overall physical and mechanical integrity of the mural appears rather well preserved [29]. Thanks to digital archive of images (Google Street View), it was possible to reconstruct the chronological evolution of the mural, in an annual time-lapse from 2014, the year of its creation, to 2022**.** The progression of the mural's appearance is documented in the supplementary materials (Supplementary Fig. S1). This reconstruction clearly shows that by June 2015 - less than a year after completion - the section of the mural depicting Mandela's face had already undergone a significant fading. In Fig. 1, the colour changes in Mandela's portrait, a general loss of contrast in the central background, and whitening [29] in the left section are evident. According to the artists' recollections and photographic documentation, the different shades of brown colours used for Mandela's face were realized by mixing different paints (unfortunately, of unknown type and supplier), while the painting materials used of the left section (Nais) consisted of Montana MTN94 spray cans, as supplied. This study guided the choices of restoration intervention, while at the same time, the expertise and knowledge of the restorer influenced both the diagnostic workflow and the accuracy of the analyses.

2. Materials and methods

2.1. Non-invasive investigations, digital documentation and sampling

Non-invasive in-situ analyses involved photographic documentation and reflectance Hyperspectral Imaging (HSI).

The mural's original state was assessed by comparing online images and balancing colours using white backgrounds of street signs as a white balance reference. HEX colour codes were obtained using Adobe Photoshop (Adobe Inc.) on balanced images, averaging the colour selection within a 900 pixels area (or at least 100 pixels for smallest areas). Detailed and calibrated (Calibrite ColourChecker Passport) photographic documentation (Nikon D750, objective Nikon AF-S 24–85 mm f/3.5–4.5 G ED VR) was used to assess colour changes. The colour simulation of paint mixtures was conducted using the software "Online colour mixing tool" (trycolors.com/mixer), exclusively using the primary colours Red (#FF0000), Yellow (#FFFF00), Blue (#0000FF), Black (#000000) and White (#FFFFFF) as mixture components. This approach was used to recreate and simulate the colour mixtures and primary colours ratios of both the mural's original and faded palettes, based on the HEX colour codes obtained from the digital documentation [40].

HSI was performed on Mandela's face portion of the mural, within a square region of 30 cm per side containing all the different brown shades. The hyperspectral camera (with sensitivity in the spectral range between 400 and 900 nm and spectral resolution of about 4 nm at 600 nm) uses a Fourier Transform approach by exploiting a TWINS (Translating-Wedge-Based Identical Pulses eNcoding System) interferometer

[1] Dr. Davide Riggiardi.

Fig. 1. a) Original appearance of the mural, photo taken immediately after the realization in 2014; b) appearance of the mural in 2022, sampling points are indicated in white.

coupled to a monochromatic camera [41]. Direct sunlight (a sunny day in early March) was used as the illumination source. To reconstruct diffuse reflectance spectral data, calibration of reflectance values was performed using an absolute-standard-white reference (Labsphere Spectralon®, >95 % total reflectance in the range 250–2500 nm) placed in the camera field-of-view. Clustering of the areas was performed through t-stochastic neighbour embedding (t-SNE) [42]. This dimensionality reduction technique visualizes high-dimensional data by mapping similar data points (spectra) close to each other in a lower-dimensional space, typically two dimensions, preserving the relationships between the points. Afterwards, a manual clustering was performed in the new two-dimensional space to identify the different groups.

Results of HSI analysis supported the selection of sampling areas. Specifically, sampling was taken from all the colour shades in Mandela's face and from some other areas of the mural exhibiting signs of colour instability (the red and blue geometrical background on the left). The samplings points analysed in this study are displayed in Fig. 1 and reported in Table 1. Samples were collected in assistance of a restorer, using a scalpel, collecting materials from the mortar up to the painting layer.

2.2. Optical and stereo microscopy

Morphologies and stratigraphy were investigated in all the samples using stereo and optical microscopy instruments, i.e., Leica M205C stereo and a Leica DM6 optical microscope coupled with an MC 150 HD and Flexacam C1 camera, respectively. Samples have been embedded in a methacrylate resin, Technovit 2000 LC (Heraeus Kulzer, Germany), to produce polished cross sections. Optical microscopy of the cross-sections guided the selection of samples for further analysis.

Table 1
List of samples collected from the mural, object of this research.

Sample code	Artist	Colour
OPB01	Orticanoodles	Purple-grey
OLB02	Orticanoodles	Light brown
ODB03	Orticanoodles	Dark brown
OB04	Orticanoodles	Beige
O06	Orticanoodles	Black and dark brown
NB10	Nais	Blue
NR11	Nais	Red

2.3. μ-FTIR spectroscopy

Micro-Fourier transform infrared spectroscopy and microimaging (μ-FTIR) were performed using a Thermo Nicolet iN10 MX spectrometer by Thermo Fischer Scientific (Massachusetts, United States) equipped with a cooled MCT/A detector. Materials were identified in transmission mode by analysing micrometric grains collected with a needle under a stereomicroscope from the surface of collected sample. These microsamples were analysed in transmission mode using a diamond anvil cell (DAC). To improve material identification, some samples were treated with a 0.1 M HCl solution to remove calcite residues that can obscure other characteristic infrared signals in the DAC spectra, following a previously reported method [13]. Spectra were acquired with 64 or 128 scans, 4 cm^{-1} of spectral resolution, in the 4000–750 cm^{-1} range.

μ-FTIR ultrafast reflectance maps were collected from approximately 1 × 0.5 cm rectangular surface areas of the samples. To expose the original (non-faded) paints, portions of the sample surfaces were gently scratched under a microscope with a scalpel. The maps collecting aperture and steps were set to 100 × 100 μm, with spectra acquired at a spectral resolution of 9 cm^{-1} using 8 scans. Multivariate curve resolution processing was applied to the reflectance spectra matrix to differentiate the spectra of the original paint (scratched surface) from those to the faded paint (untouched surface). μ-ATR FTIR single-point spectra were acquired both in the scratched and untouched areas of the surfaces to better interpret the reflectance spectra. These spectra were acquired using a slide-on μ-ATR accessory with a germanium crystal tip, with acquisition parameters set to 128 scans 4 cm^{-1} spectral resolution and collection window equal to 200 × 200 μm.

2.4. Raman spectroscopy and mapping

μ-Raman analysis was conducted using a Thermo Scientific DXR3 Raman Microscope by Thermo Fischer Scientific (Massachusetts, United States). The measurements were performed with a laser having 532 nm wavelength, 10 mW real output power and 50 μm aperture. The laser spot size was 10 μm and the grating was 400 lines/mm. The samples were observed with objectives of 50 × and 100 × . Spectra were collected in the spectral range between 3500 and 50 cm^{-1} with 2 cm^{-1} of resolution. Data were treated with the software OMNIC (Thermo Fischer Scientific, United States). SOPrano library and Scherrer et al. [43] were used as references for the identification of the pigments [44,

45].

2.5. EDXS mapping and SEM microscopy

EDXS mapping investigated elemental composition on stratigraphy. Au-metallized cross-sections were observed at high magnification by a Zeiss Supra 40 Field-Emission Scanning Electron Microscope (FE-SEM), operating in high-vacuum and equipped with the GEMINI column. The accelerating voltage was set at 20 kV. On the same samples, the elemental composition was determined by energy-dispersive X-ray spectroscopy (EDXS) by using an Xplore-15 energy dispersive spectrometer (Oxford Instruments).

3. Results and discussion

3.1. Colour palette reconstruction

Fig. 2 a and b illustrate the colour change between the original and faded states of Mandela's face. Comparing the two palettes (Fig. 2c and d), it can be noticed that the beige tone has lost saturation turning greyish; the light-brown tone colour has shifted to a different shade of brown; the purple-brown has strongly faded from a brown tone to a greyish-purple hue; and the dark-brown has lost contrast becoming lighter.

The artist declared that the different colours of Mandela's palette were created onsite by mixing different paints and colours. The different behaviour of the brown shades (some faded and others not) may be ascribed to the different composition of the paint mixture realized by artist to achieve the desired colour tones. In fact, some components in this paint mixtures may be more unstable than others, causing the observed specific tone changes. To identify the components associated to the major fading, a colour mixing software was used to simulate the composition of purple-brown colour that exhibited the most significant fading (Fig. 3). The simulated mixture of the original purple-brown colour was created using only primary colours (black, white, red, yellow and blue). By adjusting the component proportions in the simulation to match the faded purple-brown, it was possible to associate the fading with the loss of red and yellow, hence suggesting that the instability of these pigments could be responsible for the chromatic alteration (Fig. 3).

3.2. Reflectance Hyperspectral Imaging

Reflectance HSI was performed in situ on a squared area of Mandela's face (dotted box in Fig. 2b corresponding area shown in Fig. 4a). t-SNE analysis was performed on the HSI datacube to cluster the image into subareas characterized by similar spectral features. Results are provided in Fig. 4b–d on the basis of spectral similarities. This finding allowed targeted sampling by limiting it to a single sample for each

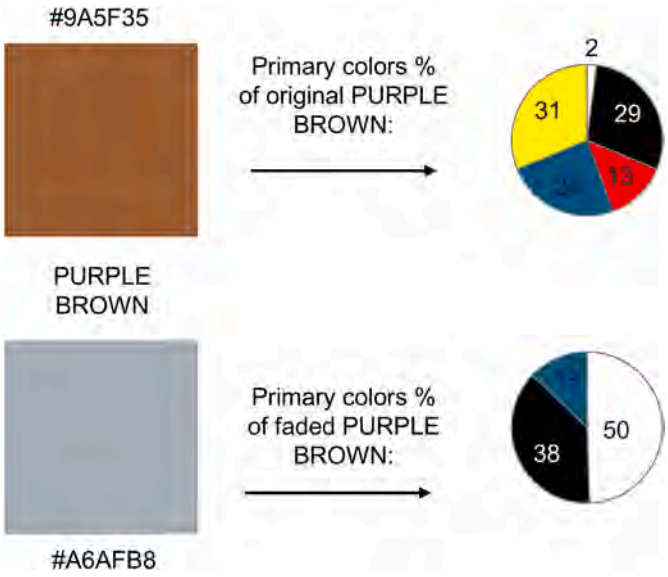

Fig. 3. Simulated colour composition of original and faded purple-brown tone. It is possible to note that the faded colour doesn't contain any yellow and red components. (For interpretation of the references to colour in this figure legend, the reader is referred to the Web version of this article.)

colour field. In addition, it is noted that reflectance spectra of beige, light brown and light beige shades (Fig. 4d) exhibit a similar spectral behaviour, which is different from that of the purple-brown, dark brown and black coloured areas (Fig. 4d), indicating that the different shades of brown have been realized by mixing the same paints (and pigments) in different proportion to achieve different brown hues. Furthermore, by looking at the first derivative with respect to the wavelength of the spectral data (Fig. 4e–f), it was revealed the presence of the drawing trace under the painting layers. In Fig. 4e the derivative map of hyperspectral data at 580 nm, is shown, where a dashed line is clearly visible, corresponding to the trace of the drawing. The artists likely used the cartoon method, similar to *spolvero*, to transfer the drawing. While *spolvero*, traditionally employed in mural paintings, uses a needle and black powders to trace the outlines of the figures, nowadays modern spray cans are employed.

3.3. Optical and stereo microscopy

Micro samples, collected from the different coloured fields (Table 1), were analysed both by stereo and optical microscopy in visible reflected light as loose fragments and on polished cross-sections.

Sample purple-brown (OPB01), coming from Mandela's face, shows

Fig. 2. a) Detail of Mandela's face from the original appearance of the mural in 2014; b) detail of faded Mandela's face in 2022; c) original colour palette from Mandela's face in 2014; d) faded colour palette from Mandela's face in 2022. The box with dashed line in b) show the area of HSI investigations reported in Fig. 4. (For interpretation of the references to colour in this figure legend, the reader is referred to the Web version of this article.)

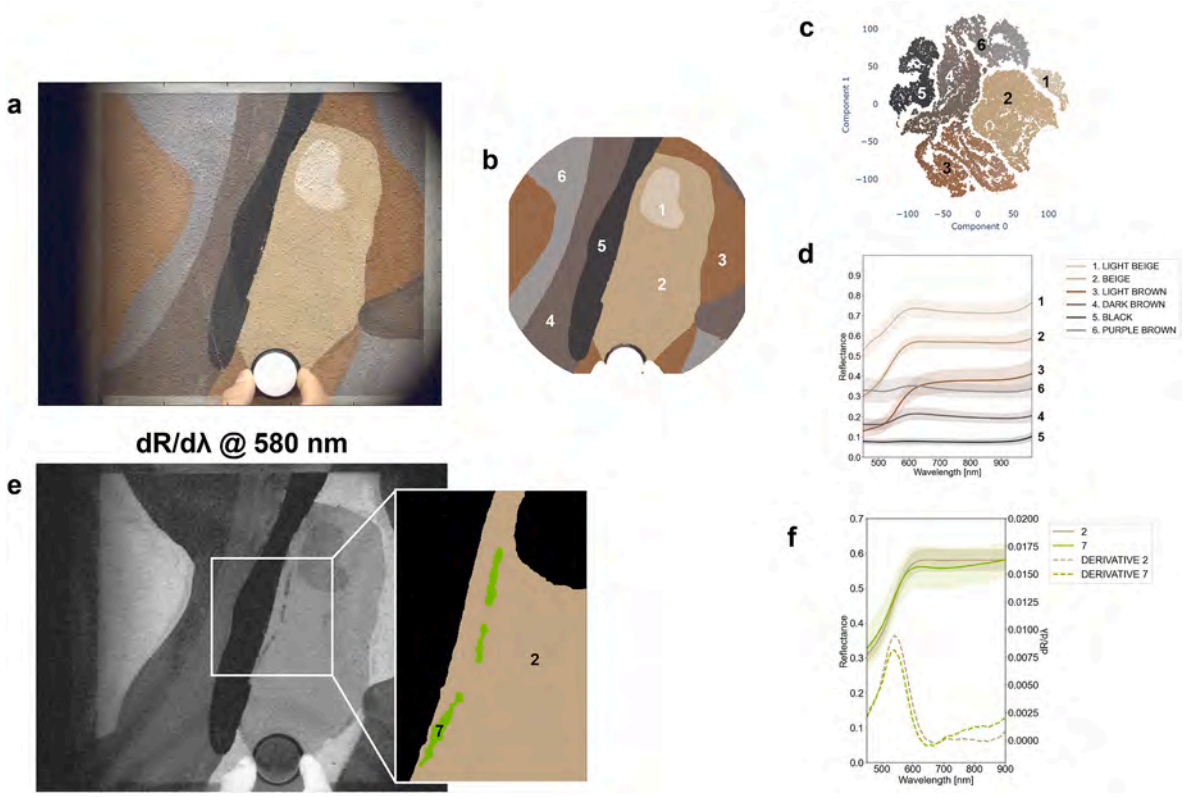

Fig. 4. (a) Colour picture of the area investigated with reflectance HSI, depicting a portion of Mandela's face. (b-d) Results of t-SNE analysis of the reflectance HSI datacube: (b) Classification map creating by clustering areas with similar spectral reflectance properties; (c) t-SNE scatterplot where each point is coloured as the relative pixel in the RGB image; (d) mean reflectance spectrum of each cluster with standard deviation. (e-f) Analysis of the first derivative: (e) Map of the first derivative at 580 nm where the dashed line (green) is visible, corresponding to the drawing trace of the artist, the inset shows the results of t-SNE clustering on this subarea; (f) mean reflectance spectrum and standard deviation of each cluster and first derivative of spectral data. (For interpretation of the references to colour in this figure legend, the reader is referred to the Web version of this article.)

a non-homogeneous surface colour appearance of the paint, with purple areas and original brown tone spots (Fig. 5a). Diffused evaporation holes along the surface are visible, from which it is possible to observe the brownish tone underneath (Fig. 5a, arrow in 10 ×). he polished cross section (Fig. 6a), shows a colour stratigraphy with the purple faded layer on top, and the original brown colour below. The faded layer is approximately 10 μm thick, while the whole painting layer (original + faded) is about 30 μm thick. A yellow primer varnish is present beneath the paint layer over a yellowish preparation mortar layer (Fig. 6a). In the UV fluorescent image, the faded superficial layer is easily distinguished from the original brown, the decayed superficial layer showing a brighter fluorescence. This could be attributed to the more fluorescent resin penetrated in that faded layer due to its loss of consistency after the decay.

Sample beige (OB04), taken from Mandela's face, has a homogeneous surface colour appearance of the paint with some evaporation holes (Fig. 5b, arrow in 20 ×). The paint seems compact and shows a glossy appearance typical of non-decayed paints (Fig. 5b). In cross-section (Fig. 6b), it is immediately visible the whitish faded layer (10 μm thick) on top of the beige paint (20 μm thick). A yellow primer varnish layer is present between the yellowish preparation mortar layer and the beige paint. In the UV fluorescent image, the white primer layer is well visible in red and no difference in fluorescence is detectable between the beige paint and the white faded layer.

For what concerns Nais' blue (NB10) sample, stereo microscopy observation shows an inhomogeneous whitish layer with some blue pigment grains dispersed in it (Fig. 5c, arrow in 20 ×). In the cross-section (Fig. 6 c), the stratigraphy shows clearly the whitish faded layer on top: this latter is about 6 μm thick, while the average thickness of blue paint is 15 μm. A white primer varnish layer is present between the yellowish preparation mortar layer and the blue paint. With UV light, the white primer layer is easily distinguished with respect to the other layers for its reddish fluorescence [33]. Nais' red (NR11) sample shows again a whitish superficial layer, that covers the red layer below. In this case, the surface painting layer seems more compact and homogeneous, but several microcracks are present on the surface. Inside these cracks, it is easily visible the vivid red paint underneath (Fig. 5d, arrow in 20 ×). In cross-sections (Fig. 6 d), the red painting layer is very thick (150 μm) with a thin yellow layer in the middle. However, this thick painting layer could be interpreted as the result of the overlapping of two red layers applied after a change of mind of the artist. The superficial degraded layer is barely detectable (3 μm) on top of the external one. A discontinuous whitish primer is visible between the yellowish mortar layer and the red paint. In UV light, the faded superficial layer is easily detected, the red-orange layer exhibits a bright red fluorescence with some filler grains showing a blueish one.

In the literature [33], this superficial white surface layer is called "chalking effect" and it is associated to the presence of a low amount of synthetic organic pigments (SOPs) on the surface of the paint and to the small pigment grain size compared to the fillers (calcite, barite, talc, etc).

Samples coming from light brown (Fig. 7a) and dark brown (Fig. 7b) show a more homogeneous surface painting layer, in colour and texture; these layers appear less deteriorated maintaining their original hues. By observing the polished cross-sections of these samples, it was confirmed the presence of a single unaltered painting layer, without surface colour fading. Fig. 7c shows the surface of a sample, taken on the border between dark brown and black colour areas, as observed through stereomicroscopy. The lateral green, roundish areas are possibly the artist's underlying drawing lines, which had been highlighted by PL-HIS

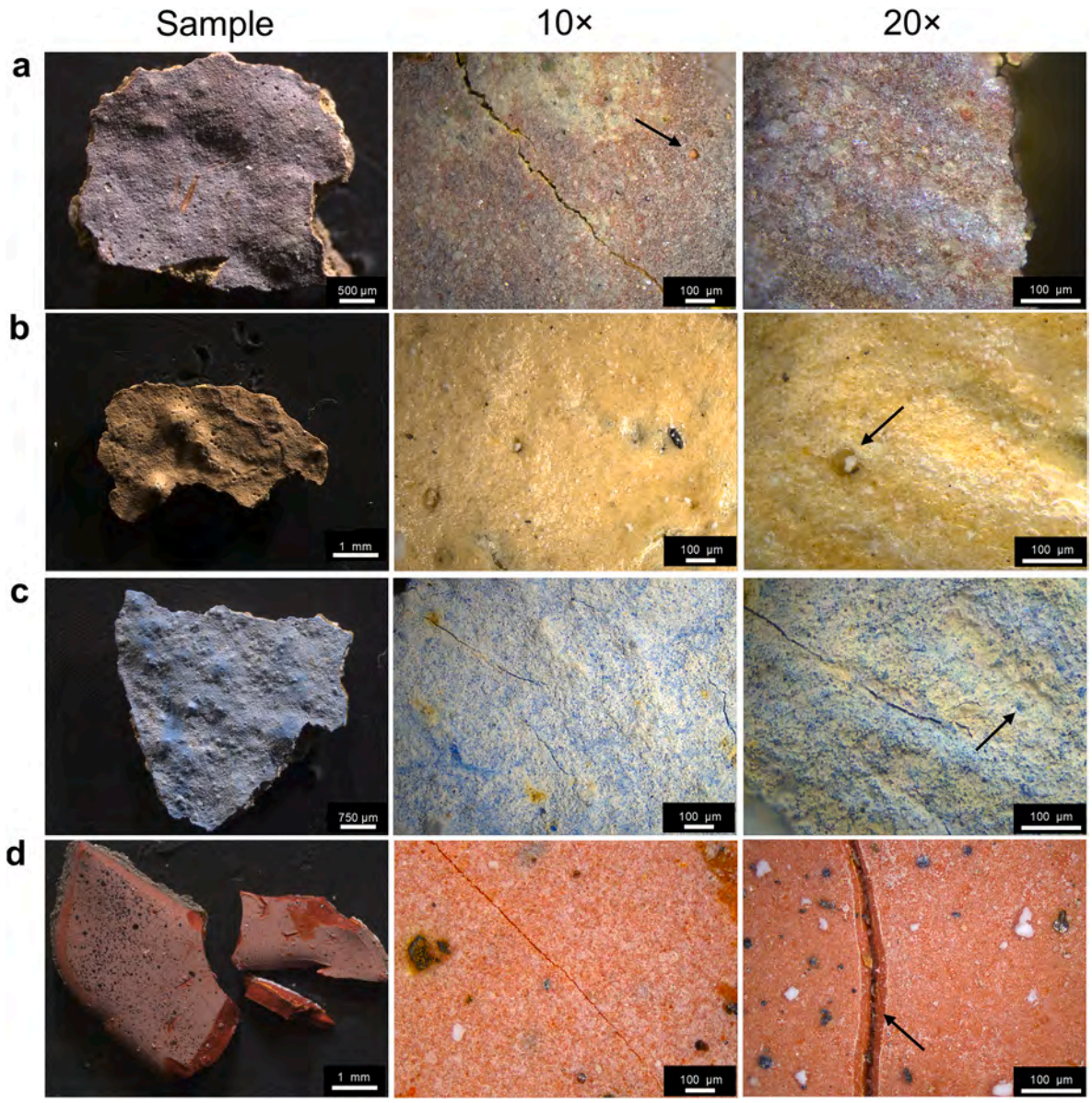

Fig. 5. Stereo and optical microscope images of: a) Purple-brown sample OPB01 and b) beige colour OB04 from Mandela's face; c) light blue sample NB10 and d) red sample NR11 from Nais's area. (For interpretation of the references to colour in this figure legend, the reader is referred to the Web version of this article.)

investigation (§3.2). The cross section confirms that this green colour is below the two painting layers and above the primer layer.

3.4. *Reflectance μ-FTIR mapping and μ-ATR FTIR*

μ-FTIR analyses allowed to define the nature of the paints, in terms of binder and additives compositions and to investigate the surface compositional differences in the faded paints. For what concerns samples from Mandela's face paint, the main binding medium was identified as a mixture of PVAc and acrylic resin (DAC μ-FTIR spectra collected from samples OPB01 and OB04). Specifically, the following bands can be assigned to the binder: 1740 cm^{-1} for the C═O stretching, 1370 cm^{-1} for C–H bending, C–O and C–C stretching at 1240 cm^{-1} and 790 cm^{-1} for C–H rocking [46,47]. OH vibrations ranging from 3695 to 3620 cm^{-1} and bands at 1114, 1030, 1010, 938, 913, 795 and 699 cm^{-1} allowed to identify the presence of kaolinite (PW19) as filler in the paint [47,48]; bands at 2513, 1795, 1417, 874 and 711 cm^{-1} are attributable to C–O stretching and C═O carbonate bond of calcite (calcium carbonate, PW18) [23]; bands at 1160, 1080, 799-780 and 695 cm^{-1} are compatible with the presence of quartz [49]. The band located at 848 cm^{-1} could be ascribed to the halo carbon compounds (Cl–C), possibly related to some synthetic organic pigment, or the presence of nitrocellulose. The identification of pigments was not possible by μ-FTIR spectroscopy.

The faded sample OPB01, which is purple-brown on the very surface, when gently scratched with the scalpel under the stereo microscope reveals the underlying original brown. Reflectance μ-FTIR imaging of the scratched surface (Fig. 8a) allows to gather, after elaboration with multivariate curve methodology, a compositional map. The obtained map shows a clear differentiation between the original and faded paint. μ-ATR FTIR single points (Fig. 8b) confirmed this difference in terms of chemical composition: in the spectrum of the faded paint, the main binder band completely disappears (band at 1740 cm^{-1}), and an enrichment of additives can be observed. The appearance of a broad band located around 1650 cm^{-1} could be related to the oxidation reaction and C═C, C═O bonds formation [50,51].

μ-FTIR reflectance maps of the superficially scratched sample OB04 (Fig. 8c) make more visible the difference between the scratched

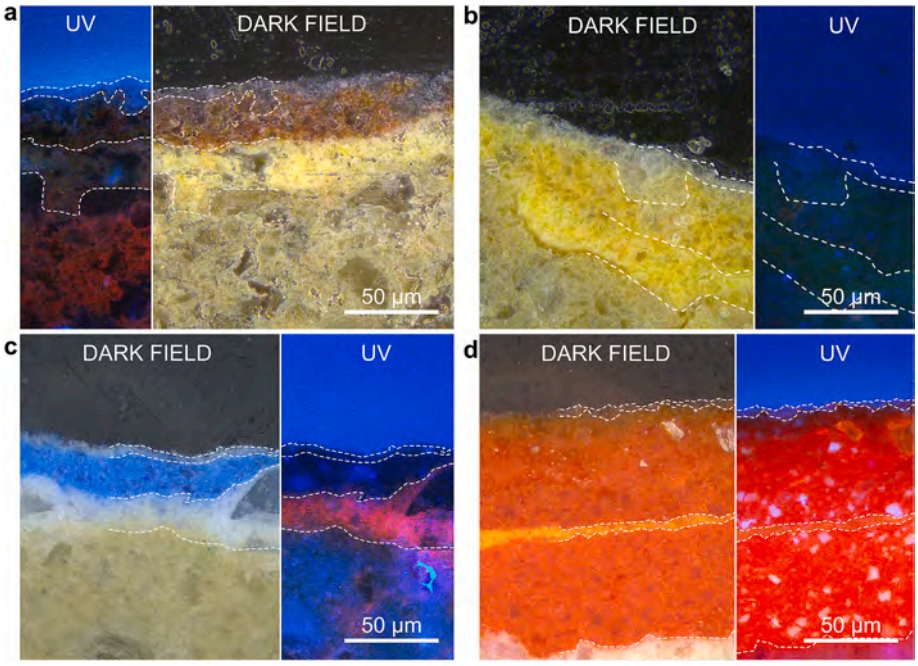

Fig. 6. VIS optical microscopic images and fluorescence microscopy images of cross sections of sample: a) OPB01, b) OB04, c) NB10 and d) NR11. The white dashed lines indicate the same areas between VIS and UV images, highlighting the stratigraphy.

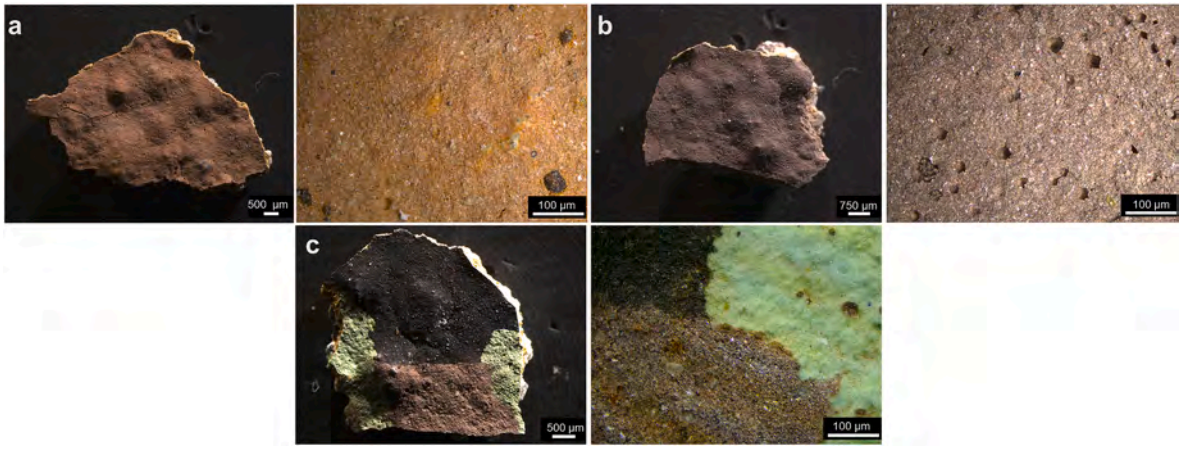

Fig. 7. Stereo and optical microscope images of samples: a) OLB02; b) ODB03; and c) O06.

(original beige layer) and faded paint areas (surface white layer), which in the visible image can be hardly distinguished. µ-ATR FTIR single points spectra (Fig. 8d) confirmed the difference in terms of chemical composition. Contrary to what was observed for the previous sample, in the degraded layers, a loss of additives and, as a consequence, an increase of the binder band intensities (1740 cm^{-1} and a better definition of the polymer fingerprint 1165, 1144 and 1113 characteristic of C–O and C–C bonds of acrylic resin [52]) were observed.

Investigations on samples from the left side of the mural (NB10 and NR11) revealed that the paint was based on an acrylic/alkyd resin binder. Binder identification was assessed by the presence of signals in the range 2960-2875, 1730 cm^{-1}. Band at 3675 (MgO/MgOH octahedral layer) and 1020 (the Si–O tetrahedral layer) cm^{-1} are related to the presence of talc as filler [53]. Band at 2513, 1795, 1420, 877 cm^{-1} are ascribed to calcite presence in sample NB10. The presence of rutile in NB10 is recognizable from the rising trend of the spectrum below 850 cm^{-1} [47]. The presence of calcium oxalates is assessed from the bands at 1635, 1320 and 782 cm^{-1} [54,55]. Finally, bands at 1119, 1090, 1060, 900, 755 and 730 cm^{-1} have been associated with the presence of phthalocyanine pigment blue (PB15, C.I.:74160) in blue sample [47] and bands at 3110, 1626, 1612, 1593, 1481, 1448, 1400, 1342, 1309, 1180, 1130, 843, 835, 758, 741 and 708 cm^{-1} with the presence of Azo pigment orange (PO5) in red sample [56].

Reflectance maps of the superficially scratched sample NB10 (Fig. 9a) match with the visible microscopic image of scratched (original blue) and untouched white (faded) areas. µ-ATR FTIR single points spectra (Fig. 9b) confirmed this difference in terms of chemical composition: in fact, in the faded layers, it can be observed the disappearance of the carbonyl bands related to the binder resin and a strong decrease of bands associated with the organic pigment (PB15). The appearance of bands at 1635 and 1317 cm^{-1} is attributed to calcium oxalate, probably formed during the degradation of the binder, most likely assisted by biological attack [55,57].

In the same way, reflectance maps of the superficially scratched sample NR11 (Fig. 9c) match with the visible microscopic image of scratched (original red) and untouched white (faded) areas. µ-ATR FTIR single points spectra (Fig. 9d) confirmed the different chemical composition in terms of the intensity and relative ratios of bands

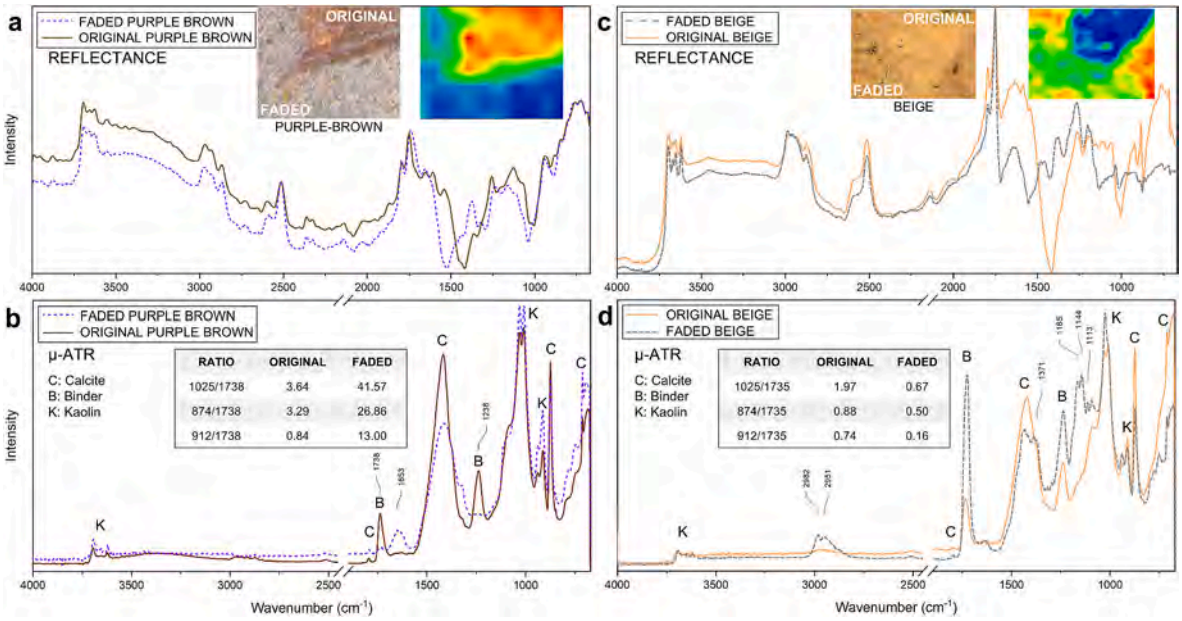

Fig. 8. μ-FTIR reflectance mapping and spectra (a–c), and μ-ATR spectra (b–d) from the sample (a–b) OPB01 and (c–d) OB04. The bands that differentiate the faded from the non-faded spectrum are highlighted and assigned to materials.

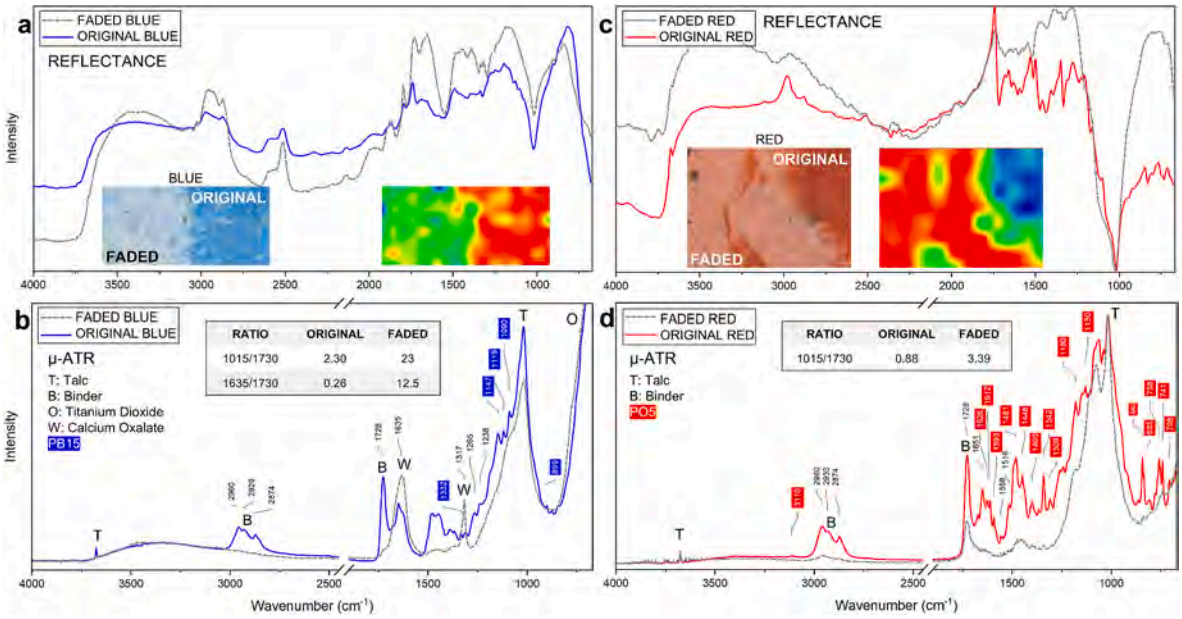

Fig. 9. μ-FTIR reflectance mapping and spectra (a–c), and μ-ATR spectra (b–d) from samples: (a–b) NB10 and (c–d) NR11. The bands that differentiate the faded from the non-faded spectrum are highlighted and assigned to materials. Bands of pigments are highlighted in coloured boxes.

ascribed to both the resin and the pigment. The ratio additive/binder increases in the faded layer. The appearance of a broad band located around 1650 cm^{-1} could be related to the oxidation reaction and C═C, C═O bonds formation [50,51].

3.5. *μ-Raman spectroscopy of polished cross-sections*

μ-Raman single point spectra were acquired from polished cross-sections of samples OPB01, OB04, NB10 and NR11. The analysis on the yellowish preparation mortar (pink line in Fig. 10a), a common element for all samples, showed the presence of chalk (calcium carbonate PW18), gypsum (PW26) and TiO_2 in rutile form (PW6) [27]. Raman results are summed up in Table 2.

Raman spectrum of the brown non-faded layer from sample OPB01 (brown in Fig. 10a) exhibits the main peaks of pigments Diarylide Yellow PY83 (1954, 1399, 1333, 1253, 955, 917, 660, 537, 395, 341, 262 cm^{-1}) and Naphthol AS Red PR112 (1483, 1357, 1289, 1230, 1160 cm^{-1}) [43,44]. Instead, in the purple-brown faded layer (purple in Fig. 10a) strong peaks of rutile (PW6) at 610, 440, 230 and 140 cm^{-1} and peaks of calcite (PW18) at 1085, 711, 280 and 153 cm^{-1} [27] have been identified. The spectrum from the yellow primer layer (yellow in Fig. 10b) matches with PY83, rutile (PW6), chalk (PW18) and gypsum (PW26). From the deconvolution of PR112 and PY83 peaks at 1388 and 1398 cm^{-1} in the brown layer spectrum (Supplementary Fig. S2), it was possible to estimate the relative amount of the two pigments in the paint, that was actually equal to the one obtained from the digital simulation

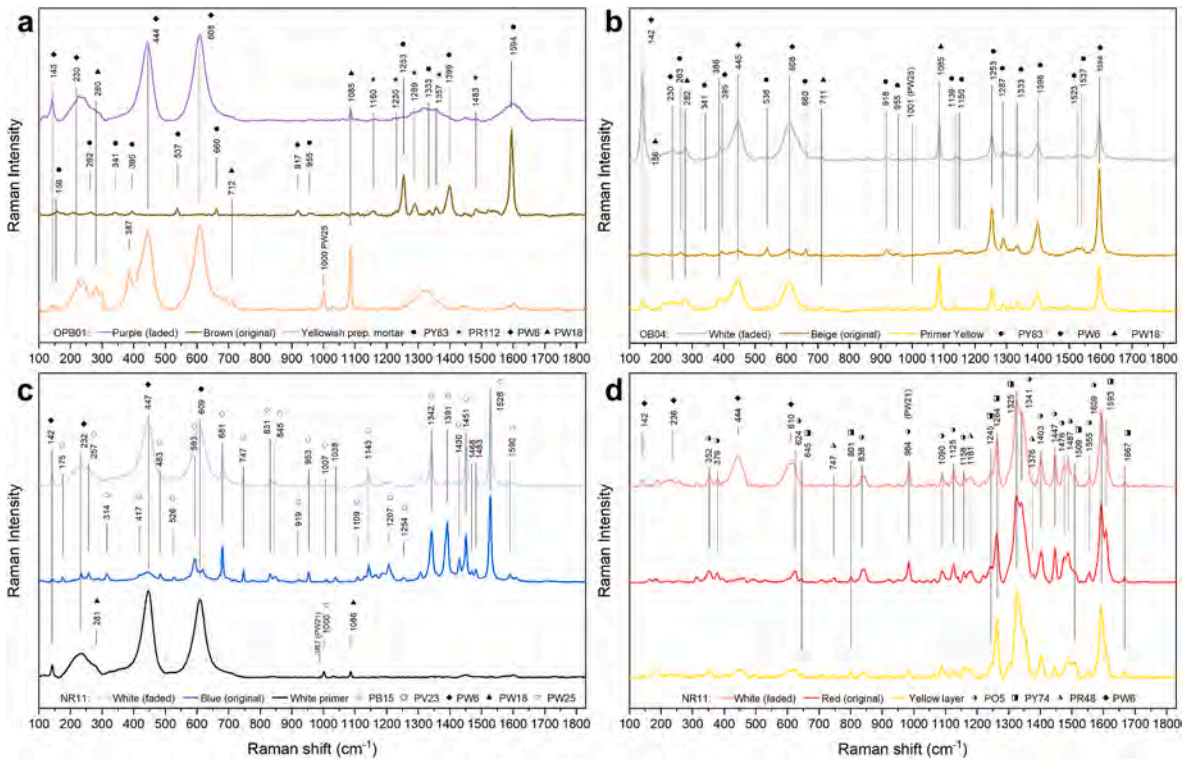

Fig. 10. Raman spectra from samples: a) OPB01, b) OB04, c) NB10, d) NR11. Yellowish preparation mortar (pink line in a) is in common with all the samples; Yellow primer layer (yellow line in b) is in common between samples OPB01 and OB04; white primer (black line in c) is in common between NB10 and NR11. Peaks are assigned to pigments and additives through specific symbols reported in each graph. (For interpretation of the references to colour in this figure legend, the reader is referred to the Web version of this article.)

Table 2
Results of μ-Raman spectroscopy and Energy dispersive X-ray spectroscopy on stratigraphies.

Sample	Layers	μ-Raman spectroscopy	EDXS mapping
OPB01	Purple faded	Chalk PW18, rutile PW6	Ca, Ti (low), Ba (low), Cl (low), Al
	Brown non-faded (original)	PR112, PY83	Ca, Ti (low), Ba (low), Cl, Al
	Yellow primer	PY83, chalk PW18, rutile PW6, gypsum PW25	Ca, Ti, Ba, Si, S, Cl, Al
	Yellowish prep. mortar	Chalk PW18, gypsum PW25, rutile PW6	Ca, Ti, Ba, Fe
OB04	White faded	PY83, chalk PW18, rutile PW6.	Ca, Ti, Ba, Si, Cl
	Beige	PY83, rutile PW6	Ca, Ti, Ba, Si, Cl
	Yellow primer	PY83, chalk PW18, rutile PW6, gypsum PW25	Ca, Ti, Ba, Si, S, Al, Cl
	Yellowish prep. mortar	Chalk PW18, gypsum PW25, rutile PW6	Ca, Ti, Ba, Fe
NB10	White faded	PB15	Ti (rich), Ba (rich), Ca
	Blue	PB15, PV23	Ti (rich), Ba (rich), Ca
	White primer	gypsum (PW25), chalk (PW18)	Ca (rich), Ti, Ba
	Yellowish prep. mortar	Chalk PW18, gypsum PW25, rutile PW6	Ca, Ti, Ba, Fe
NR11	White	PY74, PO5 and PR48, rutile PW6, barite PW21	Ti, Ba, S, Mg
	Red	PY74, PO5 and PR48	Ti, Ba, S, Mg
	Yellow thin	PY74 and barite PW21	Ti, Ba, Mg
	White primer	gypsum (PW25), chalk (PW18)	Ca, Ti, Ba
	Yellowish prep. mortar	Chalk PW18, gypsum PW25, rutile PW6	Ca, Ti, Ba, Fe

(Fig. 3) of the paint mixture (red:yellow = 0.42 while PR112:PY83 = 0.48).

Raman spectra on sample OB04 revealed the presence of PY83 and rutile (PW6) in both the beige original layer (beige in Fig. 10b) and the faded white layer (grey in Fig. 10b). However, the ratio between pigment PY83 and rutile is quite different, showing a strong decrease in the faded surface layer. In this last, the presence of rutile is much more evident. The yellow primer layer (yellow in Fig. 10b) revealed to be composed of PY83, chalk (PW18) and rutile (PW6).

Measurements on the blue paint layer (blue in Fig. 10c) from sample NB10 matched with two pigments: PB15 (Phthalocyanine Blue, maybe PB15:3) and PV23 (C.I.: 51319, Dioxazine Violet) [43,44]. The signals from PB15 were detected in the blue paint layer and the white faded layer, while those from PV23 only in the original blue paint layer. The faded layer (pale blue in Fig. 10b) shows peaks of rutile (PW6) and very weak signals from PB15. Furthermore, the white primer layer (black in Fig. 10b) shows the presence of gypsum (PW25) and chalk (PW18).

Measurements on the red paint layer of NR11 sample (red in Fig. 10d) matched with the presence of pigment PO5 (C.I.: 12075, Hansa Orange), PY74 (C.I.: 11741 Arylide Yellow) and PR48 (C.I.: 15955 Permanent Red) [43,44] In addition to them, in the faded superficial white layer (pink in Fig. 10d), the presence of rutile (PW6) was detected. The very thin yellow intermediate layer in the middle of the red one (yellow in Fig. 10d) revealed the presence of PY74 and barium sulfate (PW21). The white primer layer (black in Fig. 10b) shows the presence of gypsum (PW25) and chalk (PW18).

3.6. FE-SEM microscopy and EDXS mapping of polished cross-sections

FE-SEM observation and EDXS mapping of polished cross-sections of the same samples analysed by Raman spectroscopy were carried out with the aim of investigating the elemental composition of their stratigraphy. EDXS results are summarized in Table 2. The yellowish

preparation mortar layer, in common among all the samples, revealed to be rich in Iron (Fe), Calcium (Ca), Titanium (Ti) and Barium (Ba). Ca is present across all layers, particularly prominent in preparation and primer layers due to the presence of chalk and gypsum, as detected in μ-FTIR investigation. Ti and Ba have been always found together in most layers but varying in concentration depending on the paints; they are, most probably, due to the addition of titanium white (PW6) and barium sulfate in the painting mixture. Aluminium (Al) and Silicon (Si) are present due to the use of kaolinite as filler.

Focusing on the surface fading phenomena, in sample OPB01 (Fig. 11), the brown original layer is composed of Al, Mg (Magnesium), Ca, Ti, Ba, S (Sulfur), Si, and Cl (Chlorine). Chlorine is the element that allows to differentiate the faded surface layer from the original brown: as it is visible in Fig. 11c, Cl concentration decreases towards the surface of the cross-section. In the brown layer, EDXS confirms the presence of calcite crystals as detected by μ-FTIR.

Elemental maps from sample OB04 indicate that S allows to clearly differentiate the beige-coloured painting layer from the yellow primer, but inside the painting layer, it isn't possible to detect any elemental difference between the beige and the surface white faded layer.

EDXS results of sample NB10 show that the primer white layer is very rich in Ca and Si from mineral clasts. The presence of Ti and Ba characterizes the blue painting layer and the faded surface white layer, while no difference between the faded white layer and the original blue paint layer was detected.

Elemental maps from sample NR11 indicate that the primer white layer is based on Ca (rich), Ti and Ba (lower amount). The original red paint layer contains S, Ti, Ba and Al, showing also the presence of Mg and Si as clusters. The yellow thin intermediate layer is recognized by looking at Ti and Ba maps. No elemental difference is detected between the white faded surface layer and the original red.

3.7. Key findings and degradation mechanisms

Stratigraphic analysis revealed thin faded layers (10 μm for OPB01, purple-brown, and OB04, beige, 5 μm for NB10, blue, and NR11, red), consistent with previous findings on similar paints [16]. The photo-oxidation of the polymeric binder, revealed by μ-ATR FTIR, led to the accumulation of white fillers on the surface, producing the well-documented "chalking effect," characterized by increased roughness, light scattering, and gloss reduction [5,32,33].

Raman spectroscopy on NB10 (blue) identified increased rutile (PW6) content and a selective loss of PB15 and PV23 in faded layers, confirming that degradation primarily results from organic pigment depletion. This was further supported by μ-ATR FTIR and EDXS, which showed a homogeneous distribution of white fillers across both original and faded layers, ruling out migration processes [15–17,23,30,33]. The distinct boundary between faded and intact layers suggests that fading depth is controlled by oxygen diffusion and photodegradation kinetics, possibly influenced by volatile degradation by-products [19,31,32,35].

The degradation mechanism, schematized in Fig. 12, is driven by the combined degradation of the polymeric binder and synthetic organic pigments due to photo-oxidation and environmental exposure. As these components degrade and are progressively lost, either through volatilization or washing away by rain, the surface layer becomes depleted of both the binder and pigments. This depletion results in a relative enrichment of white fillers, such as calcite, talc, and barite, which remain embedded in the paint matrix and are responsible for the observed whitening effect.

The most striking case is OPB01 (purple-brown), where EDXS revealed a significant loss of Cl in the faded layer, correlating with the disappearance of PY83 and PR112, two chlorine-containing pigments (Supplementary Fig. S3) [32,43]. Digital simulations confirmed that this pigment loss caused a dramatic colour shift from brown to faded purple-brown, significantly altering Mandela's portrait. These findings align with previous reports of PR112 poor outdoor stability [14].

4. Conclusions

The contemporary mural painting "*20 Years of Freedom and Democracy*" was subjected to a fast chromatic alteration in about 2 years and an impactful colour fading within a decade from the realization. Analyses showed that fading phenomena is only a surface phenomenon. The chalking effect with an evident whitening of the painted surfaces, contributes to the colour changing, due to the deterioration of the polymeric binding phases of paints, the loss of pigments particles and a clear enrichment of white fillers on the surface. This leads to a general loss of contrast in the artists' palettes. Sometimes, the instability and loss of specific pigments (in our case study, yellow and red pigments) induce a dramatic change of colour and tones, that compromises the reading and appearance of the mural.

The results of this study can induce restorers to elaborate a new conservation proposal, removing the very surface deteriorated layers at the aim of recovering the original tones. Actually, the microscopic observations of the cross-sections highlighted that the fading phenomenon affects approximately 10 μm, or less, of the superficial painting materials. The challenge could be the set-up of an appropriate "cleaning" methodology that allows only the removal of very thin faded layers. After eight years of outdoor exposure, it was observed that about one-third of the average thickness of the painting layers (around 30 μm) had been affected. Therefore, it would be beneficial to assess whether the degradation process shows a stable kinetic over time. In the scenario of an ongoing process with a constant rate of deterioration, and in the case of periodic cleaning involving the removal of degraded paint, it can be postulated that the complete loss of the artwork, due to excessive thinning of the paint layers, would be reached in about 20 years.

A better understanding of colour fading phenomena, their chemical nature, key environmental factors and evolution over time, is indispensable for appropriate conservation strategies. Nevertheless, the intrinsic weakness of paints and the extremely aggressive urban environment should induce conservators and scientists together, to develop new protective materials and careful maintenance strategies, at the aim of conserving this diverse artistic open-air patrimony.

CRediT authorship contribution statement

Nicolò Guarnieri: Writing – original draft, Visualization, Methodology, Investigation, Formal analysis, Data curation, Conceptualization.

Fig. 11. Microscopic observation of sample OPB01: a) FE-SEM image at 2250 × magnification; b) optical microscopy VIS image; c) EDXS map of Cl counts.

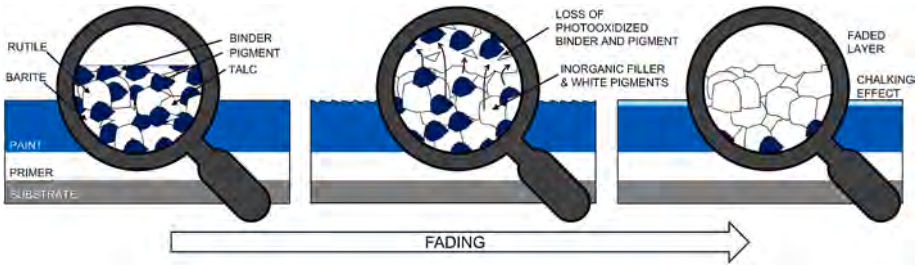

Fig. 12. Scheme of the hypothesized mechanism for the surface whitening phenomenon. The creation of the faded layer is associated with the degradation and loss of organic materials (binder and SOPs) and accumulation at the surface of white inorganic pigments and fillers.

Alessia Di Benedetto: Writing – review & editing, Validation, Investigation, Data curation. **Daniela Comelli:** Writing – review & editing, Investigation. **Francesco Mirani:** Writing – review & editing, Investigation. **David Dellasega:** Writing – review & editing, Investigation. **Laura Pagnin:** Writing – review & editing, Visualization, Investigation, Data curation. **Sara Goidanich:** Writing – review & editing, Supervision, Project administration, Methodology, Investigation, Conceptualization. **Lucia Toniolo:** Writing – review & editing, Supervision, Project administration, Methodology, Investigation, Funding acquisition, Data curation, Conceptualization.

Funding

This research was funded by the PRIN2020 project "SUPERSTAR -Sustainable Preservation Strategies for Street Art" (2022–2025), Prot. 2020MNZ579, an Italian collaborative project, https://prin2020superstar.dcci.unipi.it/funded by the Italian Ministry of University and Research (MUR).

Alessia Di Benedetto PhD research was financially supported by the European Union's NextGenerationEU Programme with the I-PHOQS Infrastructure [IR0000016, ID D2B8D520, CUP B53C22001750006] "Integrated infrastructure initiative in Photonic and Quantum Sciences.

Declaration of competing interest

The authors declare the following financial interests/personal relationships which may be considered as potential competing interests: Sara Goidanich reports financial support was provided by Italian Ministry of University and Research (MUR) PRIN2020 project 2020MNZ579. If there are other authors, they declare that they have no known competing financial interests or personal relationships that could have appeared to influence the work reported in this paper.

Acknowledgements

The Authors are deeply grateful to Dr. Davide Riggiardi, for providing the important case study and for his invaluable knowledge, assistance and conservation expertise during the experimental work onsite, and express their gratitude to artists for their generous availability and cooperation to the reconstruction of the mural's details. The Authors would like to express their sincere gratitude to Dr. Nicolò Cellamare for his invaluable assistance with the digital photographic processing and his valuable contribution to the research work.

Appendix. ASupplementary data

Supplementary data to this article can be found online at https://doi.org/10.1016/j.dyepig.2025.112733.

Data availability

Data will be made available on request.

References

[1] Pagnin L, et al. Protecting street art from outdoor environmental threats: what are the challenges? Coatings Dec. 2023;13(12). https://doi.org/10.3390/coatings13122044. Art. no. 12.
[2] Cadetti A. Conservare la street art: le problematiche del muralismo contemporaneo in Italia. Firenze: Edifir edizioni Firenze; 2020.
[3] Rivaroli L, et al. Mural art conservation data recording (SCIMA): the graart. Project 2021;4(4). https://doi.org/10.3390/heritage4040232. Heritage.
[4] Bruni R, Rauhut Kompaniets O. Street art and place-making of villages: examples of Italian painted villages. JPMD; Aug. 2024. https://doi.org/10.1108/JPMD-09-2023-0097.
[5] Cimino D, et al. Assessing the (In)Stability of urban art paints: from real case studies to laboratory investigations of degradation processes and preservation possibilities. Heritage Mar. 2022;5(2):581–609. https://doi.org/10.3390/heritage5020033.
[6] Molodid O, et al. Research for banksy mural "judoki" in BORODYANKA. Int J Conserv Sci Dec. 2023;14(4):1381–90. https://doi.org/10.36868/IJCS.2023.04.08.
[7] Shpakova H, et al. Structural and technological aspects of conservation of street art on buildings damaged during the war. Int J Conserv Sci Feb. 2024;15(SI):103–18. https://doi.org/10.36868/IJCS.2024.si.09.
[8] Mezzadri P. Contemporary murals in the street and urban art field: critical reflections between preventive conservation and restoration of public art. Heritage Sep. 2021;4(3). https://doi.org/10.3390/heritage4030142. Art. no. 3.
[9] Collina A, et al. A dialogue between two worlds: the conservation of Poesia DI. VINO by Ivan Tresoldi. J Cult Herit May 2022;55:11–7. https://doi.org/10.1016/j.culher.2022.02.003.
[10] Rivas T, et al. Forms and factors of deterioration of urban art murals under humid temperate climate; influence of environment and material properties. Eur. Phys. J. Plus Nov. 2022;137(11):1257. https://doi.org/10.1140/epjp/s13360-022-03473-1.
[11] Germinario G, et al. Integrated investigations to study the materials and degradation issues of the urban mural painting ama il tuo sogno by jorit agoch. Sustainability Jan. 2024;16(12). https://doi.org/10.3390/su16125069. Art. no. 12.
[12] La Nasa J, et al. A chemical study of organic materials in three murals by Keith Haring: a comparison of painting techniques. Microchem J Jan. 2016;124:940–8. https://doi.org/10.1016/j.microc.2015.06.003.
[13] Cucci C, et al. The colors of keith haring: a spectroscopic study on the materials of the mural painting tuttomondo and on reference contemporary outdoor paints. Appl Spectrosc Jan. 2016;70(1):186–96. https://doi.org/10.1177/0003702815615346.
[14] Magrini D, et al. A multi-analytical approach for the characterization of wall painting materials on contemporary buildings. Spectrochim Acta Mol Biomol Spectrosc Feb. 2017;173:39–45. https://doi.org/10.1016/j.saa.2016.08.017.
[15] Dickens J, et al. Keith haring in pisa and Melbourne: controversy and conservation. Stud Conserv Jun. 2016;61(sup2):29–37. https://doi.org/10.1080/00393630.2016.1193691.
[16] Bosi A, et al. Street art graffiti: discovering their composition and alteration by FTIR and micro-Raman spectroscopy. Spectrochim Acta Mol Biomol Spectrosc Jan. 2020;225:117474. https://doi.org/10.1016/j.saa.2019.117474.
[17] Rousaki A, et al. An in-and-out-the-lab Raman spectroscopy study on street art murals from Reggio Emilia in Italy. Eur. Phys. J. Plus Feb. 2022;137(2). https://doi.org/10.1140/epjp/s13360-022-02423-1. Art. no. 2.
[18] Sabatini F, et al. Fluorescent paints in contemporary murals. A Case Study Aug. 2023;6(8):5689–99. https://doi.org/10.3390/heritage6080299. Heritage.
[19] Marazioti V, et al. The condition of contemporary murals in sun-exposed urban environments: a model study based on spray-painted mock-ups and simulated light ageing. Heritage Aug. 2024;7(8). https://doi.org/10.3390/heritage7080186. Art. no. 8.
[20] Pozo-Antonio JS, et al. Deterioration of graffiti spray paints applied on granite after a decade of natural environment. Sci Total Environ Jun. 2022;826:154169. https://doi.org/10.1016/j.scitotenv.2022.154169.
[21] Sanmartín P, Pozo-Antonio JS. Weathering of graffiti spray paint on building stones exposed to different types of UV radiation. Constr Build Mater Mar. 2020;236:117736. https://doi.org/10.1016/j.conbuildmat.2019.117736.

[22] Aguilar-Rodríguez P, et al. Unexpected behavior of commercial artists' acrylic paints under UVA artificial aging. Microchem J Jan. 2021;160:105743. https://doi.org/10.1016/j.microc.2020.105743.
[23] Alonso Villar EM, et al. Resistance to artificial daylight of paints used in urban artworks. Influence of paint composition and substrate. Prog Org Coating May 2021. https://doi.org/10.1016/j.porgcoat.2021.106180.
[24] Cianci C, et al. Formulation of a new sustainable hybrid coating for the conservation of street-art: characterization and application. Prog Org Coating 2025;200. https://doi.org/10.1016/j.porgcoat.2024.109026.
[25] Melchiorre Di Crescenzo M, et al. The use of waterborne paints in contemporary murals: comparing the stability of vinyl, acrylic and styrene-acrylic formulations to outdoor weathering conditions. Polym Degrad Stabil Sep. 2014;107:285–93. https://doi.org/10.1016/j.polymdegradstab.2013.12.034.
[26] Gwardzińska-Chowaniec Ż, et al., editors. Urban art and what next? the issues of preservation of contemporary art. Warszawa: academy of fine arts in warsaw. first ed.; 2021.
[27] La Nasa J, et al. 60 years of street art: a comparative study of the artists' materials through spectroscopic and mass spectrometric approaches. J Cult Herit Mar. 2021;48:129–40. https://doi.org/10.1016/j.culher.2020.11.016.
[28] Alonso-Villar EM, et al. Sol-silicate versus organic paints: durability after outdoor and ultraviolet radiation exposures. Prog Org Coating Jul. 2022;168:106843. https://doi.org/10.1016/j.porgcoat.2022.106843.
[29] project CAPuS. Glossary from CAPuS project [Online]. Available: http://www.capusproject.eu/glossary/; 2020.
[30] Alonso-Villar EM, et al. Efficacy of colour protectors in urban art paintings under different conditions: from a real mural to the laboratory. Heritage Apr. 2023;6(4):3475–98. https://doi.org/10.3390/heritage6040185.
[31] Pellis G, et al. A multi-analytical approach for precise identification of alkyd spray paints and for a better understanding of their ageing behaviour in graffiti and urban artworks. J Anal Appl Pyrolysis Aug. 2022;165:105576. https://doi.org/10.1016/j.jaap.2022.105576.
[32] Anghelone M, et al. Spectroscopic methods for the identification and photostability study of red synthetic organic pigments in alkyd and acrylic paints. Microchem J Jun. 2018;139:155–63. https://doi.org/10.1016/j.microc.2018.02.029.
[33] Anghelone M, et al. Photostability and influence of phthalocyanine pigments on the photodegradation of acrylic paints under accelerated solar radiation. Polym Degrad Stabil Dec. 2017;146:13–23. https://doi.org/10.1016/j.polymdegradstab.2017.09.013.
[34] van Driel BA, et al. Determination of early warning signs for photocatalytic degradation of titanium white oil paints by means of surface analysis. Spectrochim Acta Mol Biomol Spectrosc Feb. 2017;172:100–8. https://doi.org/10.1016/j.saa.2016.04.026.
[35] Krmpotić M, et al. Study of UV ageing effects in modern artists' paints with MeV-SIMS. Polym Degrad Stabil Jan. 2022;195:109769. https://doi.org/10.1016/j.polymdegradstab.2021.109769.
[36] Cortea IM, et al. Characterization of spray paints used in street art graffiti by a non-destructive multi-analytical approach. Color Res Appl 2021;46(1):183–94. https://doi.org/10.1002/col.22561.
[37] Mandela mural in milan celebrates South Africa's 20 years of democracy – nelson Mandela foundation. https://www.nelsonmandela.org/news/entry/mandela-mural-in-milan-celebrates-south-africas-20-years-of-democracy. [Accessed 17 June 2024].
[38] Mandela. Paopao's website. https://www.paopao.it/it/street-art/977-mandela.html. [Accessed 17 June 2024].
[39] Pao, Ivan e compagni: 8 mani per il murale di Mandela. la Repubblica; Jun. 17, 2024. Accessed: Mar. 27, 2023, https://milano.repubblica.it/cronaca/2014/07/17/foto/pao_nais_ivan_e_noodles_murale_a_otto_mani_per_mandela-91782390/1/.
[40] Online color mixing tool. https://trycolors.com/mixer. [Accessed 16 May 2024].
[41] Perri A, et al. Hyperspectral imaging with a TWINS birefringent interferometer. Opt. Express, OE May 2019;27(11):15956–67. https://doi.org/10.1364/OE.27.015956.
[42] Alfeld M, et al. Joint data treatment for Vis–NIR reflectance imaging spectroscopy and XRF imaging acquired in the Theban Necropolis in Egypt by data fusion and t-SNE. C R Phys 2018;19(7):625–35. https://doi.org/10.1016/j.crhy.2018.08.004.
[43] Scherrer NC, et al. Synthetic organic pigments of the 20th and 21st century relevant to artist's paints: Raman spectra reference collection. Spectrochim Acta Mol Biomol Spectrosc Aug. 2009;73(3):505–24. https://doi.org/10.1016/j.saa.2008.11.029.
[44] Soprano. https://soprano.kikirpa.be/. [Accessed 27 February 2023].
[45] Fremout W, Saverwyns S. Identification of synthetic organic pigments: the role of a comprehensive digital Raman spectral library. J Raman Spectrosc 2012;43(11):1536–44. https://doi.org/10.1002/jrs.4054.
[46] Pintus V, et al. Accelerated UV ageing studies of acrylic, alkyd, and polyvinyl acetate paints: influence of inorganic pigments. Microchem J Jan. 2016;124:949–61. https://doi.org/10.1016/j.microc.2015.07.009.
[47] Marazioti V, et al. Chemical characterisation of artists' spray-paints: a diagnostic tool for urban art conservation. Spectrochim Acta Mol Biomol Spectrosc Apr. 2023;291:122375. https://doi.org/10.1016/j.saa.2023.122375.
[48] Chércoles Asensio R, et al. Analytical characterization of polymers used in conservation and restoration by ATR-FTIR spectroscopy. Anal Bioanal Chem Dec. 2009;395(7):2081–96. https://doi.org/10.1007/s00216-009-3201-2.
[49] Pięta E, et al. Application of ATR-FTIR mapping to identification and distribution of pigments, binders and degradation products in a 17th century painting. Vib Spectrosc Jul. 2019;103:102928. https://doi.org/10.1016/j.vibspec.2019.102928.
[50] De Sousa M. Ramos Félix Silva, Analytical study of accelerated light ageing and cleaning effects on acrylic and PVAc dispersion paints used in Modern and Contemporary Art. Valencia (Spain): Universitat Politècnica de València; 2011. https://doi.org/10.4995/Thesis/10251/13829.
[51] França De Sá S, et al. Tracing poly(vinyl acetate) emulsions by infrared and Raman spectroscopies: identification of spectral markers. Polymers Jan. 2021;13(21). https://doi.org/10.3390/polym13213609. Art. no. 21.
[52] Pagnin L, et al. SO2- and NOx- initiated atmospheric degradation of polymeric films: morphological and chemical changes, influence of relative humidity and inorganic pigments. Microchem J May 2021;164:106087. https://doi.org/10.1016/j.microc.2021.106087.
[53] Marzbani P, et al. Surface modification of talc particles with phthalimide: study of composite structure and consequences on physical, mechanical, and optical properties of deinked pulp. Bioresources Aug. 2016;11(4):8720–38. https://doi.org/10.15376/biores.11.4.8720-8738.
[54] Kovala-Demertzi D, et al. Pigment identification in a Greek icon by optical microscopy and infrared microspectroscopy. J Cult Herit Jan. 2012;13(1):107–13. https://doi.org/10.1016/j.culher.2011.06.003.
[55] Zoppi A, et al. Metal oxalates in paints: a Raman investigation on the relative reactivities of different pigments to oxalic acid solutions. Anal Bioanal Chem May 2010;397(2):841–9. https://doi.org/10.1007/s00216-010-3583-1.
[56] IRUG Spectrum IOD00229, Pigment Orange 5 (PO5), β-Naphthol, Azo, CI12075. http://www.irug.org/jcamp-details?id=748 (accessed Jul. 07, 2024).
[57] Monico L, et al. Non-invasive identification of metal-oxalate complexes on polychrome artwork surfaces by reflection mid-infrared spectroscopy. Spectrochim Acta Mol Biomol Spectrosc Dec. 2013;116:270–80. https://doi.org/10.1016/j.saa.2013.06.084.